FERMILAB-PUB-79-118-E

EXPERIMENTAL COMPARISON OF NEUTRINO, ANTINEUTRINO, AND MUON VELOCITIES*

George R.Kalbfleisch

Fermi National Accelerator Laboratory, Batavia, Illinois 60510

Neil Baggett+ and Earle C.Fowler

Purdue University, West Lafayette, Indiana 47907

and

Joshua Alspector†

Brookhaven National Laboratory, Upton, New York 11973

ABSTRACT

No energy dependence of the velocities of neutrinos or antineutrinos is observed within the statistical and systematic errors over the energy range 30 to 200 GeV. The velocity differences (95% confidence level) are: $|\beta_\nu - \beta_{\bar{\nu}}| < 0.7\times10^{-4}$, $|\beta_{\nu_k} - \beta_{\nu_\pi}| < 0.5\times10^{-4}$ and $|\beta_{\nu(\bar{\nu})} - \beta_\mu(\text{corrected})| = |\beta_{\nu(\bar{\nu})} - 1| < 0.4\times10^{-4}$, where $\beta=v/c$.

In Fermilab experiments[1,2] to measure the interaction cross sections of neutrinos and antineutrinos from pion decay (ν_π and $\bar{\nu}_\pi$) and from kaon decay (ν_k and $\bar{\nu}_k$), we have found that these neutrinos and antineutrinos have velocities which differ from those of energetic muons penetrating the shielding by no more than one part in 10^4 (95% confidence level [CL]). Correcting for a systematic

---

*Work supported by the U.S.Department of Energy.

+Currently at Division of High Energy Physics, U.S.Department of Energy, Washington, DC 20545.

†Now at Bell Laboratories, Murray Hill, New Jersey 07974.

bias in the flight path of the penetrating muons we find that $\left|\beta_{\nu(\bar{\nu})}-1\right| < 0.4\times10^{-4}$ (95% CL) from a sample of some 9800 events. This result is a factor of ten improvement over our earlier result based on one hundred events.[3] If neutrinos are indeed massless,[4] it is expected that they move at the speed of light.[5] However since neutrinos are so vastly different from the other known particles, this expectation must be experimentally checked.[6] This paper reports the results of a significant test.

The experiment used the Fermilab narrow band neutrino beam discussed several times previously (see e.g., Ref. 2). The data come from neutrino runs with the momentum of the positive hadron beam set to 80, 130, 190 and 250 GeV, and from antineutrino runs with the momentum of the negative hadron beam set to 130, 190 and 230 GeV. Each run gives a sample of pion neutrinos and a sample of kaon neutrinos. For almost all of the data, time of flight information for the hadrons, the decay muons and the neutrino and antineutrino interactions was recorded. We use the fact that the precise spacing of proton bunches in the accelerator yields one nanosecond pulses of secondaries at intervals of 18.83 nanoseconds. If all products (secondaries from interactions, decays, etc.) travel with the same speed, this timing pattern is maintained. Our procedure is described in more detail in reference 3. That discussion is not repeated here. We wish to present here a final understanding of the timing analysis and the results obtained.

The velocity comparison of neutrinos and penetrating muons was obtained from temporally interleaved sets of data: the times of muons arising from neutrino interactions in the detector (events), and the times of muons penetrating the muon shield and the neutrino detector (decay muons). This local time comparison required an intermediate timing reference since the neutrino and muon occurrences are not simultaneous. There were typically one neutrino event and one penetrating muon recorded every ten accelerator pulses.

The experimental setup is shown schematically in Fig. 1. The 53.1 MHz rf signal from the accelerator was used as the primary intermediate reference. The time of the event (or decay muon) was measured by two counters, T3 and T2, imbedded in the detector. Two secondary timing references, MU and PI, were also used in order to understand the signal responses and the drifts and shifts which occurred during the sixty day data taking period. The MU signal was obtained by combining together the signals from four of the eight five-fold muon telescopes located downstream of the secondary dump at the end of the 350 meter decay space. The PI signal was obtained from a counter in the hadron beam coming through a small hole in this same dump.

Various timing combinations between the five signals, rf, MU, PI, T3 and T2, yield the intrinsic response and drift times given in Table I. For example, the MU-PI timing difference was stable as a function of time throughout the data taking apart from a shift due to one change in high voltage for PI. The small size of the drift deviations in Table I show this stability. Also, the widths of T3-rf, T2-rf and T3-T2 difference distributions determine the response times of T3 and T2 shown in Table I.

Over the sixty days of operation of the experiment, a number of shifts in the timing occurred due to changes in the accelerator tuning, electronic changes (and failures) and cabling changes. The data were sorted into chronological groups of data such that the energy of the beam and all of the timing distributions remained consistent. Twenty-two such groups resulted. For example, retuning of the accelerator resulted in seven shifts of rf, typically of ±1.2 ns during the course of the experiment. The MU signal was absolutely stable. The T3 and T2 signals showed shifts after down times of the accelerator or the detector, due to small changes occurring upon turn-off/turn-on of the high voltage supplies for these counters. Since the basic timing technique is the local comparison (inside each of the twenty-two chronological and consistent sets of

timing data) of the neutrino events relative to the penetrating muons, these shifts do not have any influence on the velocity differences (unless undetected). Any undetected shifts must be small and are covered in the deviations given in Table I.

However, in order to display the data in a uniform manner the average shift of each signal in each of the chronological groups from an arbitrarily chosen standard (channel 100 of time digitizer) was applied to the signals. In this way the various timing distributions may be summed and displayed over arbitrary subgroups of the data. One such plot, representing about forty percent of all the data is shown in Fig. 2. The time displayed is the difference in T2 relative to rf in nanoseconds. The open area (labeled "EVENTS") represents the time distribution for muons arising from neutrino and antineutrino interactions in a specified fiducial region of the detector. The shaded region (labeled "DECAY MUONS") is the same distribution for penetrating muons in the same cross sectional area of the detector as the neutrino events arising from decays in the 350 meter decay space upstream. The cross-hatched region is the distribution for a dimuon subsample.[7] Gaussian curves, centered on zero time, with a standard deviation of 1.1 ns (the combined value of the T2 and rf deviations given in Table I) are drawn over the data. Note that the (neutrino and antineutrino) events are displaced slightly faster than the Gaussian curve whereas the penetrating muons are displaced slightly slower. Also note that the distributions are nicely Gaussian out to three standard deviations.

The means and standard deviations of the various timing distributions are computed for each neutrino energy (ν_π, $\bar{\nu}_\pi$, ν_k and $\bar{\nu}_k$), for the closed momentum slit (wide band background) runs, and for the dimuon sample. The corresponding velocity differences averaged over (T3-rf) and (T2-rf) can then be computed as presented in Table II along with the statistical data for each sample. These differences are also shown in Fig. 3, plotted against the average neutrino

energy $\bar{E}_{\nu,\bar{\nu}}$. Note that all the velocity differences $(\beta_{\nu(\bar{\nu})}-\beta_{\mu})$ are positive and non-zero corresponding to the displacements previously noted in Fig. 2. This effect is interpreted as a bias due to the fact that the penetrating muons travel a slightly longer distance from target to detector, due to multiple scattering, than the straight line path of the neutrinos. The bias is estimated below to be $(+0.5^{+0.2}_{-0.1})\times10^{-4}$ and is shown as the dashed line and shaded region in Fig. 3.

The penetrating muons have a mean energy of about 30 GeV exiting the decay shield roughly independent of the secondary hadron energy. Allowing for the 500 meters of (mainly) earth shielding between the exit and the decay region, the mean muon energy entering the shield is about 200 GeV. At the lower energy settings, the penetrating muons arise from the small high momentum tail of the beam momentum distribution. Multiple scattering of the muons in the shield corresponds to that of an average energy of 80 GeV. A possible muon trajectory is sketched in Fig. 1. The muons scatter to some mean radius from the central beam line near the end of the decay shield. A small fraction of these muons receive a large multiple scattering back towards the detector. The mean square angle, $(\overline{\theta^2})^{\frac{1}{2}}$ for the penetrating decay muons as observed in the detector is 0.024 to 0.032 radian[8] for the various subsamples with no obvious correlation with the energy setting of the beam. Extrapolating the average muon trajectory in the detector back into the shielding along the mean angles, we find that they intersect the mean multiple scattered trajectories from the target about 100 to 120 meters from the downstream end of the shield at a radius of about three meters. This radius is about the same size as the width of the shield. The muon flight path along this trajectory is then some 0.03 to 0.06 meters longer than a straight line path to the detector and corresponds to the estimated bias given above, in Table II, and shown in Fig. 3. We see that the data points overlap with the shaded region. The other possible bias, the velocity difference of the muons with respect to light, is negligible.[9] We assume that charged muons behave as expected from special relativity.[10]

The data of Table II and Fig. 3 appear to show a (linear) rise with increasing neutrino energy $E_{\nu,\bar{\nu}}$. A best fit line is $(0.3\pm0.1)+(0.003\pm0.001)E_{\nu}$ parts per 10^4. A higher order polynomial would give a less significant slope parameter. However, in the absence of a definite reason to choose a linear deviation and in view of the spread of uncertainty of the shaded bias region, this line is not sufficiently different from a constant value to be significant.[11] Thus, taking the data to be consistent with a constant value, and correcting for the bias, where applicable, we obtain, averaging over energy, the additional entries in Table II,

$$\left|\beta_{\nu(\bar{\nu})}-\beta_{\mu}(\text{corrected})\right| = \left|\beta_{\nu(\bar{\nu})}-1\right| < 0.4\times10^{-4} \text{ (95\% CL)},$$

$$\left|\beta_{\nu_k}-\beta_{\nu_\pi}\right| < 0.5\times10^{-4} \text{ (95\% CL)},$$

$$\text{and } \left|\beta_{\nu}-\beta_{\bar{\nu}}\right| < 0.7\times10^{-4} \text{ (95\% CL)}.$$

The dimuon subsample is also consistent with these values and thus consistent with the interpretation that they mainly arise from neutrino interactions (charm production and/or secondary pion or kaon decays) rather than some slow ($\beta<1$) heavy lepton source. Unfortunately no timing information is available for neutral current events.

It is a pleasure to acknowledge the support of Fermilab and its staff, and of our home institutions. We thank our California Institute of Technology-Fermilab-Rockefeller collaborators, and especially Professor Frank Scuilli, for allowing us to extend our earlier analysis[3] into other neutrino and antineutrino samples, and for supplying us with the identity of the events in the dimuon sample.

References and Footnotes

[1] Ratio of Charged Current Cross Sections of Pion and Kaon Neutrinos Near 80 GeV, G.R.Kalbfleisch, et al, Neutrinos 78 International Conference on Neutrino Interactions and Neutrino Astrophysics, Purdue University (E.C.Fowler, Editor, April 28-May 2, 1978) p. 951.

[2]B.C.Barish, et al, Phys.Rev.Letters 39, 1595 (1977).

[3]J.Alspector, et al, Phys.Rev.Letters 36, 837 (1976).

[4]Mass limits for ν_π, see E.V.Schrum and K.O.H.Ziock, Phys.Lett. 37B, 114 (1971) and G.Backenstoss, et al, Phys.Lett. 43B, 539 (1973); and for ν_k, see A.R.Clark, et al, Phys.Rev. D9, 533 (1974).

[5]Apart from a possible very slight difference in the effective indices of refraction experienced by photons and neutrinos passing through empty space due to their differing (electromagnetic versus weak) interactions with fluctuations of the physical vacuum.

[6]G.R.Kalbfleisch, BNL Informal Report No. 20227 (unpublished).

[7]Only 65 of the 119 di- and trimuons (B.C.Barish, et al, Phys.Rev.Letters 39, 981 1977) fall in our fiducial region and within one of the twenty-two data sets mentioned in the text.

[8]The (T3 and T2) times of the muons in the detector were corrected for the observed angle of the actual trajectories observed. The mean correction was negligible (about 0.02 ns); a small number of events had corrections of 0.5-2 ns.

[9]The expected bias due to the observed $\bar{E}_\mu \gtrsim 30$ GeV corresponds to $(1-\beta_\mu) \lesssim 6\times10^{-6}$.

[10]Upper limits on the deviation of the velocity of electrons, pions, kaons and protons from the expectations of special relativity are discussed in Ref. 6 (see also footnote 1 of Ref. 3). In addition, a conservative upper limit on the muon velocity can be inferred from the differential Cerenkov studies of the composition of the hadron beams in our experiment. The muon rate downstream of an iron absorber was 0-30% higher than that calculated from the measured pions and kaons. It is believed that the excess is due to pions missing the iron absorber and causing coincidences by directly registering in the (aligned) photomultipliers on the muon counters. In any case, the "muon" pressure curve is found to be essentially identical to the pion curve. These muons (mostly from pion decay) have a momentum >0.5 that of the pions. For the 80 GeV hadron setting, the

muons have $(1-\beta) \lesssim 4\times10^{-6}$ from the "muon" pressure curve obtained in this experiment (not published). This is to be compared with $(1-\beta) < 3\times10^{-6}$ expected for $E_\mu > 40$ GeV.

[11] A two standard deviation (or less) variation of the best fit line (to; e.g., $(0.4+0.002\ E_\nu)\times10^{-4}$) would place it within the band of the estimated bias.

TABLE I

TIMING RESOLUTION

SIGNAL	$\sigma_{RESPONSE}$(ns)	σ_{DRIFT}(ns)
rf	$\lesssim$0.5[a]	$\lesssim$0.4
MU	0.6-1.0[b]	$\lesssim$0.2
PI	1.6	0.3
T3	1.3 (0.5[c])	0.4
T2	1.0	0.6

a - Thus width of proton bunch is $\lesssim$1.2 ns.

b - Varies due to rate and spill effects.

c - Slewing of time-averaged signal (measured with cosmic rays as a function of position; see Footnote 7, Reference 3).

TABLE II

VELOCITY DIFFERENCES

SAMPLE	$\bar{E}_{\nu_i}$ (GeV)	NEUTRINO EVENTS	DECAY MUONS	$\beta_{\nu_i}-\beta_\mu$ (10^{-4})	$\lvert\beta_{\nu_i}-\beta_\mu\rvert$ (95% CL) (10^{-4})	$\lvert\beta_{\nu_i}-\beta_{\bar{\nu}_i}\rvert$ (95% CL) (10^{-4})
+ 80 ν_π	32	1480	1998	0.3±0.2	<0.6	-
+130 ν_π	44	476	46	0.7±0.7	<2.1	<1.6
-130 $\bar{\nu}_\pi$	45	437	639	0.4±0.2	<0.8	
+190 ν_π	59	2085	1037	0.4±0.2	<0.7	<1.8
-190 $\bar{\nu}_\pi$	58	1223	1505	1.3±0.4	<2.1	
+250 ν_π	69	906	1102	0.4±0.2	<0.8	<0.9
-230 $\bar{\nu}_\pi$	64	782	2723	0.7±0.2	<1.1	
+ 80 ν_k	90	303	a	0.6±0.3	<1.2	-
+130 ν_k	120	121	a	0.6±0.7	<2.0	<1.7
-130 $\bar{\nu}_k$	125	195	a	0.4±0.3	<1.1	
+190 ν_k	170	1015	a	0.6±0.2	<1.0	<1.3
-190 $\bar{\nu}_k$	157	225	a	1.0±0.4	<1.8	
+250 ν_k	195	519	a	1.1±0.3	<1.8	<1.0
-230 $\bar{\nu}_k$	183	112	a	1.1±0.4	<1.9	
Background	26	38	150	1 ±1	<3	-
Dimuons	b	65[c]	b	1.3±0.8	<3	-
Bias	$\bar{E}_\mu$=23-37	-	-	$0.5^{+0.2}_{-0.1}$	-	-
All ($\nu_i+\bar{\nu}_i$)	-	9879	9050	-	<0.4[d]	<0.7
ν_k vs ν_π		2490/7286	9050	-	$\lvert\beta_{\nu_k}-\beta_{\nu_\pi}\rvert$	<0.5×10^{-4} (95% CL)

a - same as for corresponding ν_π sample.

b - covers all $\bar{E}_\nu$ <200 GeV and all penetrating decay muons.

c - one is a trimuon.

d - $\lvert\beta_{\nu(\bar{\nu})}-\beta_\mu(\text{corrected})\rvert=\lvert\beta_{\nu(\bar{\nu})}-1\rvert$ (95% CL); i.e., corrected for bias (see text) assuming $(\beta_\nu-\beta_{\bar{\nu}})=0$.

Figure Captions

Figure 1. A schematic drawing of the experimental layout. 400 GeV protons are incident on an aluminum target. Focusing and bending magnets form sign- and momentum-selected parallel secondary beams of pions, kaons and other particles. The neutrinos and muons are produced by decays of pions and kaons as they traverse the 345 meter evacuated decay pipe. Most hadrons are absorbed in the secondary dump. The neutrinos and a few energetic muons penetrate the 500 meter earth and steel shield in front of the detector. The five timing signals, rf, MU, PI, T3 and T2, arise from the detectors indicated. Also shown is a representative trajectory of a decay muon in the shield and its angle ($\theta\mu$) in the neutrino detector. SEM, XIC, DIC and $\check{C}$ are other monitors used in the experiment.

Figure 2. Timing distributions of the T2 signals relative to the rf signal for neutrino and antineutrino charged current interactions (open areas, labeled "EVENTS"), muons penetrating the shielding and the detector (shaded area, labeled "DECAY MUONS") and a sample of dimuon neutrino interactions. (The outer histogram is the sum of EVENTS and DECAY MUONS.) The curves drawn through the data are Gaussians centered on zero time with a standard deviation of 1.1 ns appropriate to the T2-rf timing difference (see text). Note the shifts of the data samples relative to the Gaussian curves.

Figure 3. The neutrino (antineutrino)-penetrating muon velocity differences of Table II versus neutrino energy $E_{\nu,\bar{\nu}}$. The dashed line and shaded area represent the estimated timing bias of the penetrating muons due to multiple scattering in the shield. The dark vertical bar at the origin represents the maximum possible bias due to other sources (see, e.g., footnote 9).

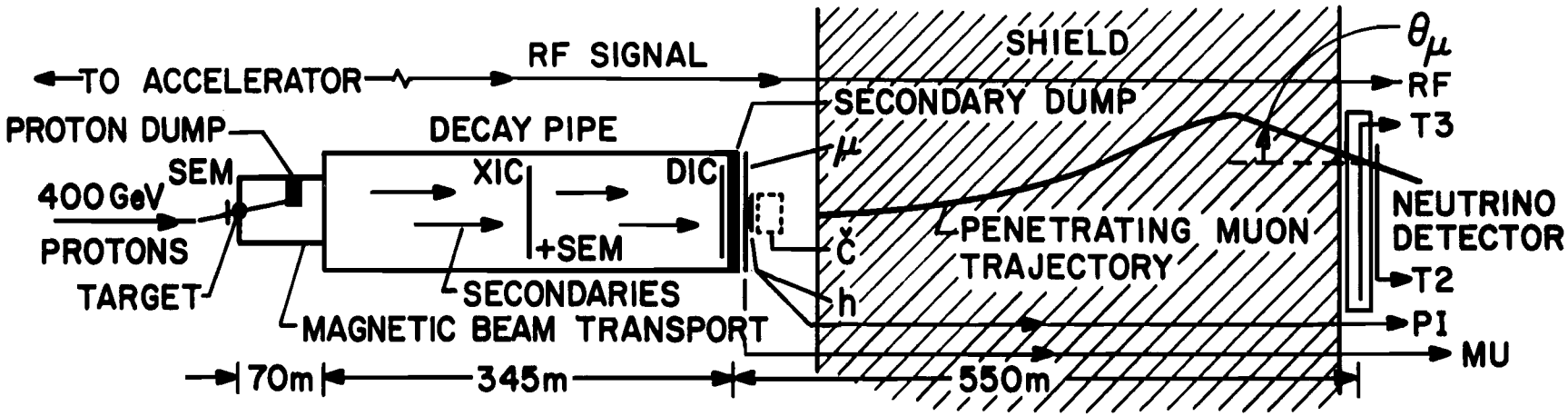
TO ACCELERATOR
RF SIGNAL
SHIELD
θ_μ
RF
SECONDARY DUMP
PROTON DUMP
DECAY PIPE
μ
T3
SEM
XIC
DIC
400 GeV
PROTONS
+SEM
$\check{C}$
PENETRATING MUON
TRAJECTORY
NEUTRINO
DETECTOR
TARGET
SECONDARIES
h
T2
MAGNETIC BEAM TRANSPORT
PI
MU
70m
345m
550m

Figure 1

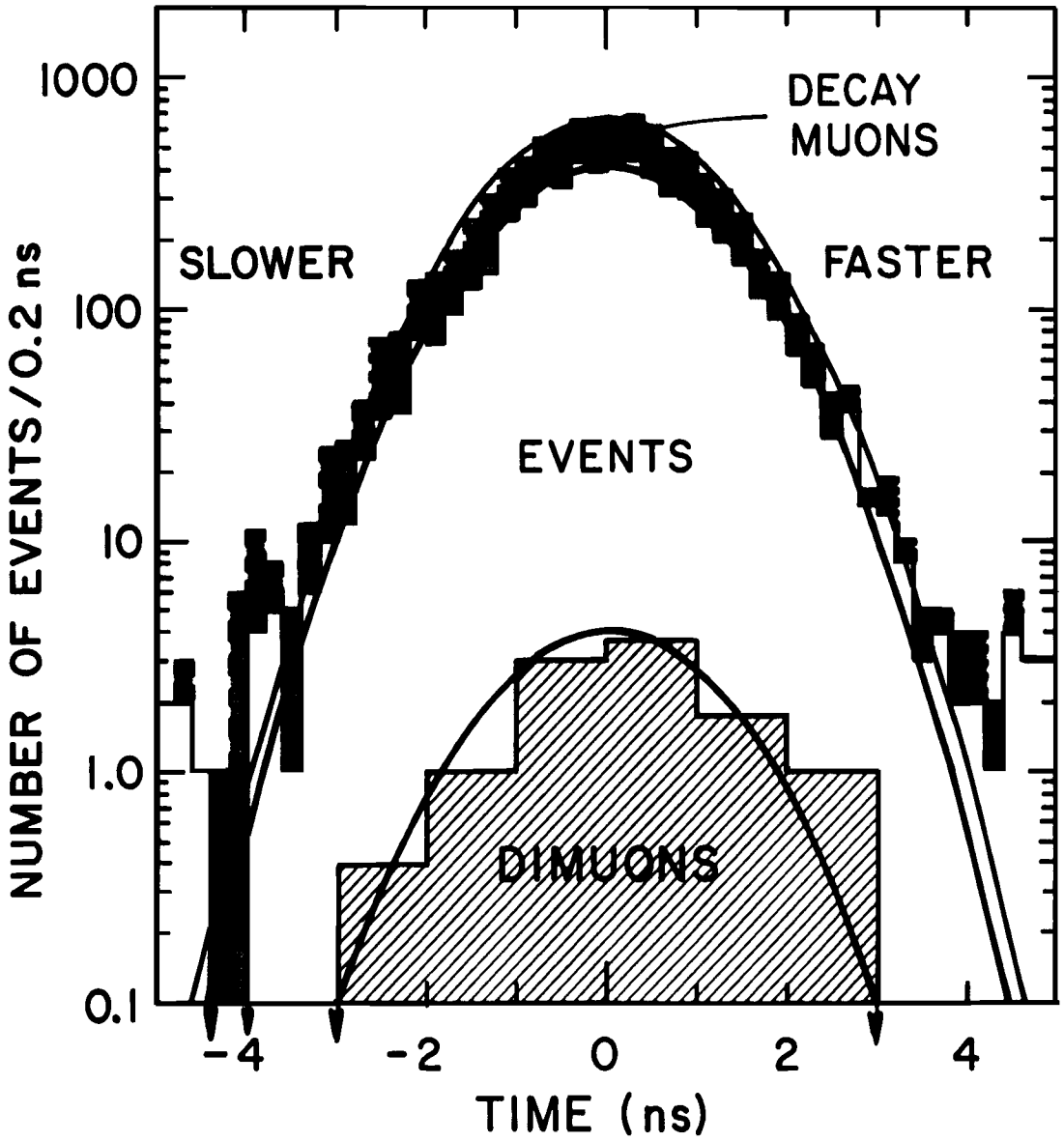
1000
100
10
1.0
0.1
NUMBER OF EVENTS/0.2 ns
DECAY
MUONS
SLOWER
FASTER
EVENTS
DIMUONS
-4
-2
0
2
4
TIME (ns)

Figure 2

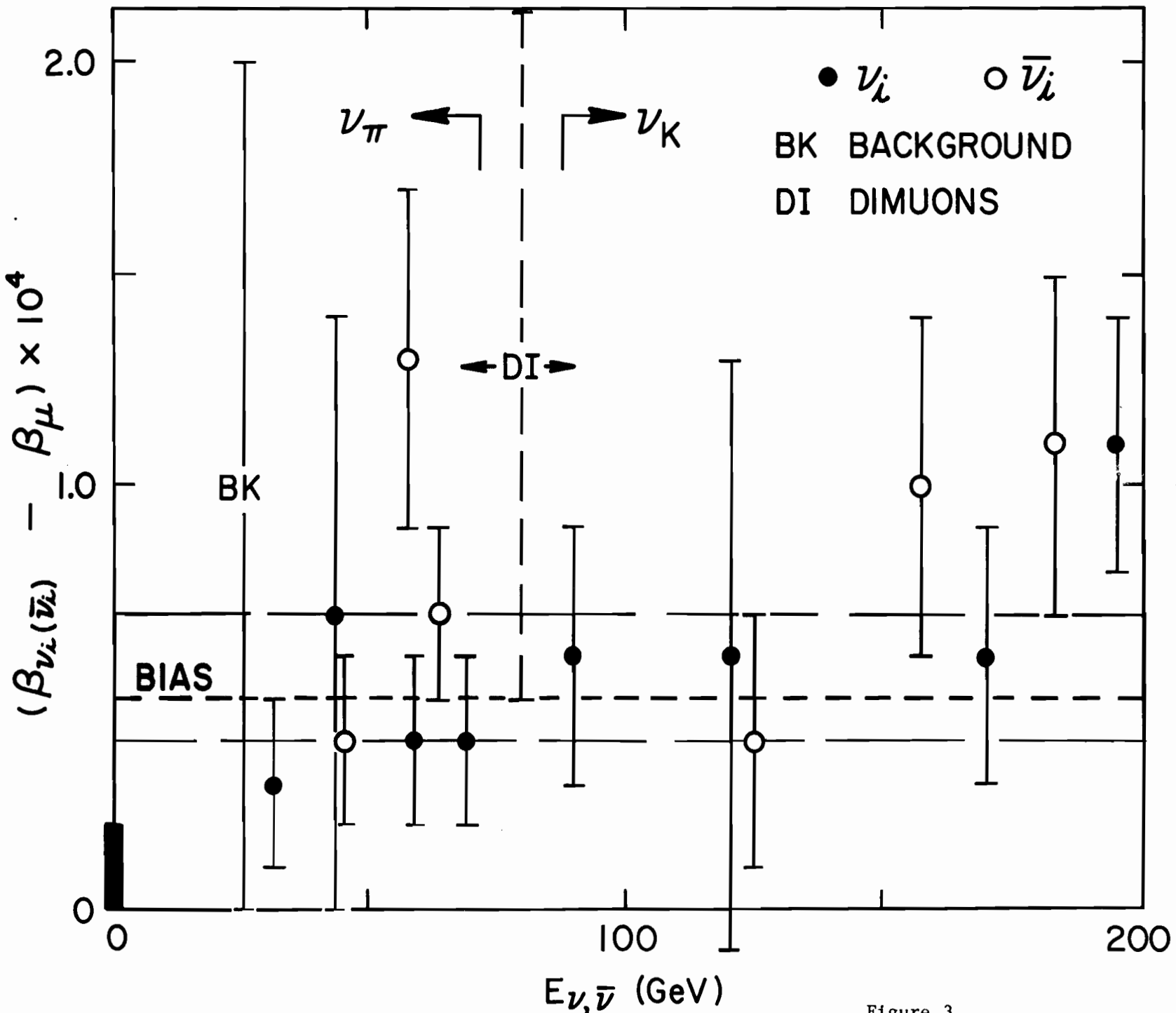
2.0
1.0
0
0
100
200
$E_{\nu,\bar{\nu}}$ (GeV)
$(\beta_{\nu_i(\bar{\nu}_i)} - \beta_\mu) \times 10^4$
ν_π
ν_K
ν_i
$\bar{\nu}_i$
BK BACKGROUND
DI DIMUONS
BK
DI
BIAS

Figure 3